

## Supporting information

### Tuning the carrier scattering mechanism to effectively improve the thermoelectric properties

#### Content list

1. Scattering mechanism in NbFeSb;
2. Comparison of electrical conductivity between  $\text{Mg}_{3.2}\text{Sb}_{1.5}\text{Bi}_{0.5}$  and  $\text{Mg}_{3.1}\text{Nb}_{0.1}\text{Sb}_{1.5}\text{Bi}_{0.5}$ ;
3. Thermoelectric properties of  $\text{Mg}_{3.2}\text{Sb}_{1.5}\text{Bi}_{0.5-x}\text{Te}_x$ ;
4. XRD of  $\text{Mg}_{3.2}\text{Sb}_{1.5}\text{Bi}_{0.5-x}\text{Te}_x$ ;
5. XRD of  $\text{Mg}_{3.2-x}\text{Nb}_x\text{Sb}_{1.5}\text{Bi}_{0.49}\text{Te}_{0.01}$  ( $x = 0.025, 0.05, 0.075, 0.10$ );
6. Band structure calculation;
7. Measurement for output power density;

## 1. Scattering mechanism in NbFeSb

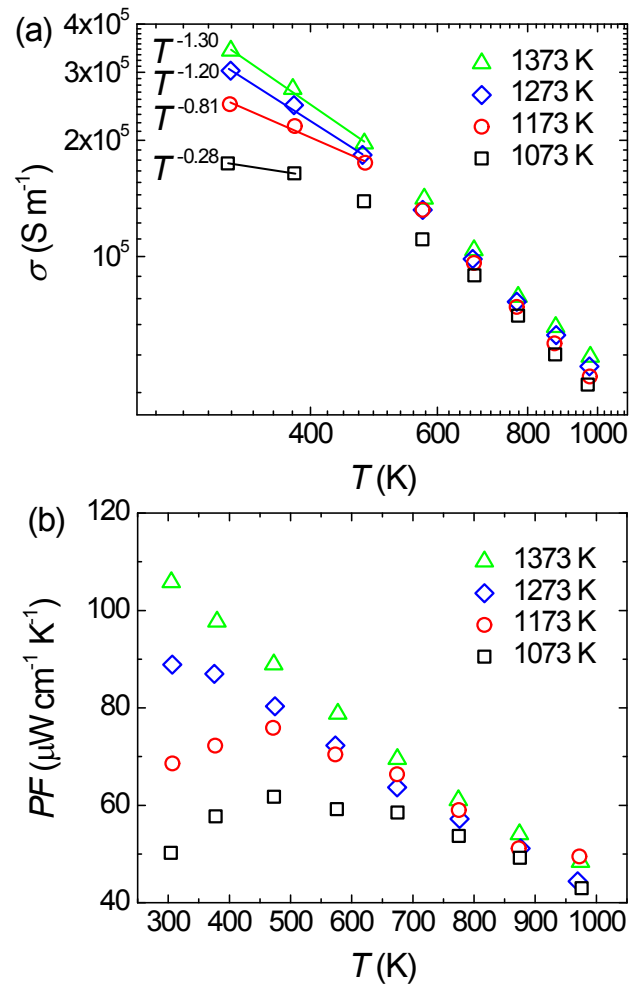


Figure S1. Temperature dependent (a) electrical conductivity and (b)  $PF$  of NbFeSb.

---

2. Comparison of electrical conductivities between  $\text{Mg}_{3.2}\text{Sb}_{1.5}\text{Bi}_{0.5}$  and  $\text{Mg}_{3.1}\text{Nb}_{0.1}\text{Sb}_{1.5}\text{Bi}_{0.5}$ ;

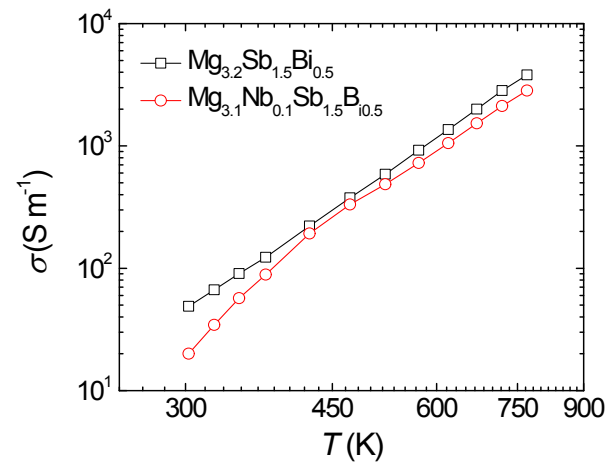


Figure S2. Comparison of electrical conductivity between  $\text{Mg}_{3.2}\text{Sb}_{1.5}\text{Bi}_{0.5}$  and  $\text{Mg}_{3.1}\text{Nb}_{0.1}\text{Sb}_{1.5}\text{Bi}_{0.5}$

### 3. Thermoelectric properties of $\text{Mg}_{3.2}\text{Sb}_{1.5}\text{Bi}_{0.5-x}\text{Te}_x$

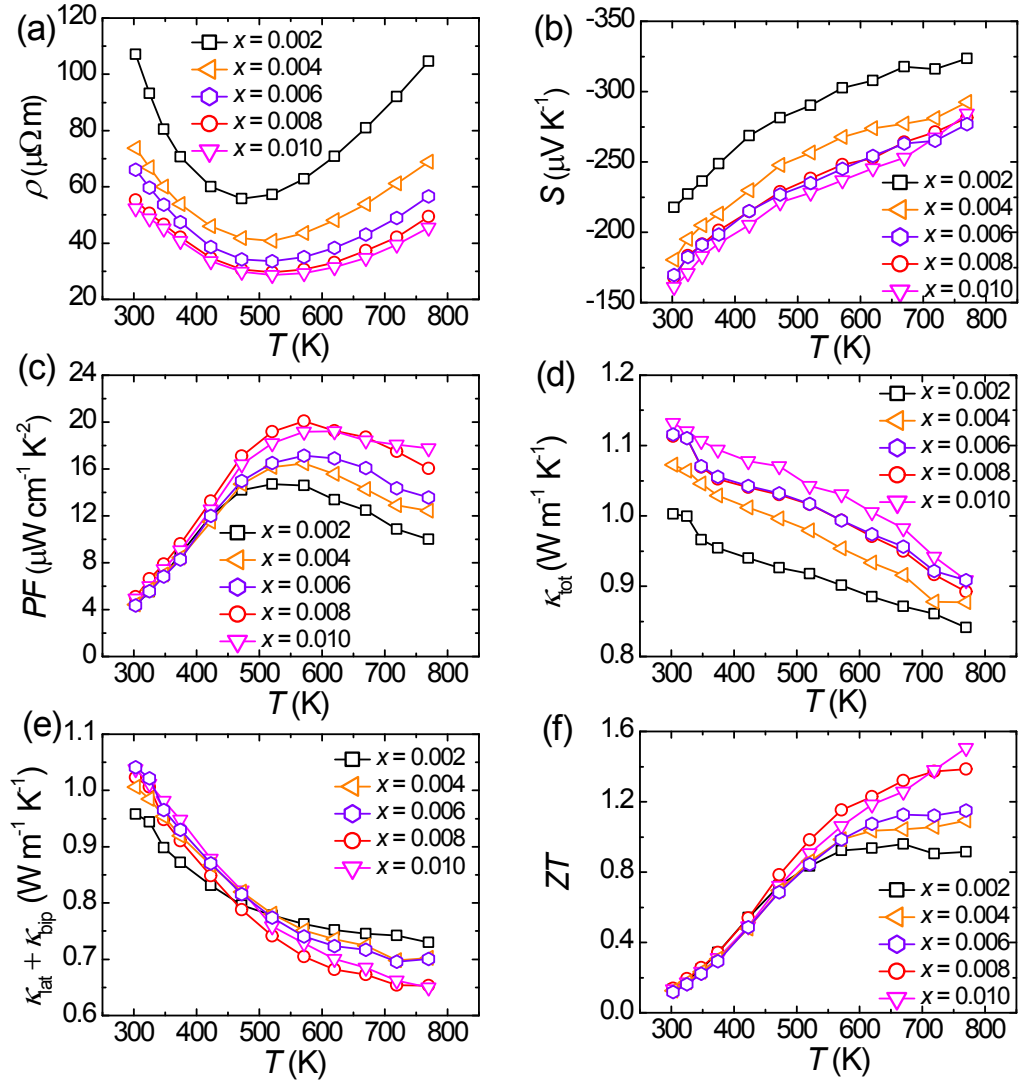


Figure S3. Temperature and composition dependent thermoelectric properties of  $\text{Mg}_{3.2}\text{Sb}_{1.5}\text{Bi}_{0.5-x}\text{Te}_x$  ( $x = 0.002, 0.004, 0.006, 0.008, \text{ and } 0.010$ ). (a) Electrical resistivity, (b) Seebeck coefficient, (c) power factor, (d) thermal conductivity, (e) sum of lattice and bipolar thermal conductivity, and (f) figure of merit,  $ZT$ .

#### 4. XRD of $\text{Mg}_{3.2}\text{Sb}_{1.5}\text{Bi}_{0.5-x}\text{Te}_x$

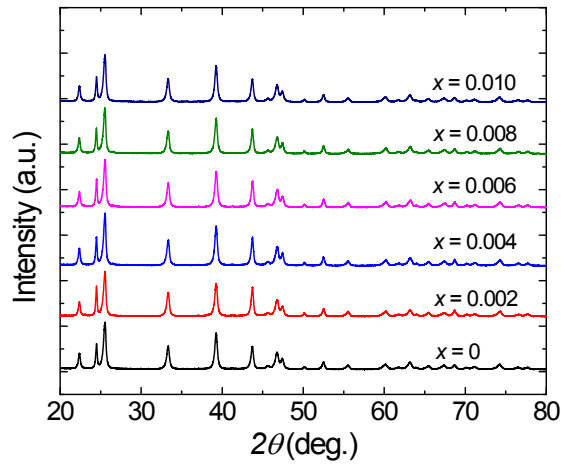


Figure S4. XRD patterns of  $\text{Mg}_{3.2}\text{Sb}_{1.5}\text{Bi}_{0.5-x}\text{Te}_x$  ( $x = 0, 0.002, 0.004, 0.006, 0.008, \text{ and } 0.010$ ).

#### 5. XRD of $\text{Mg}_{3.2-x}\text{Nb}_x\text{Sb}_{1.5}\text{Bi}_{0.49}\text{Te}_{0.01}$ ( $x = 0, 0.01, 0.05, 0.10, 0.15$ )

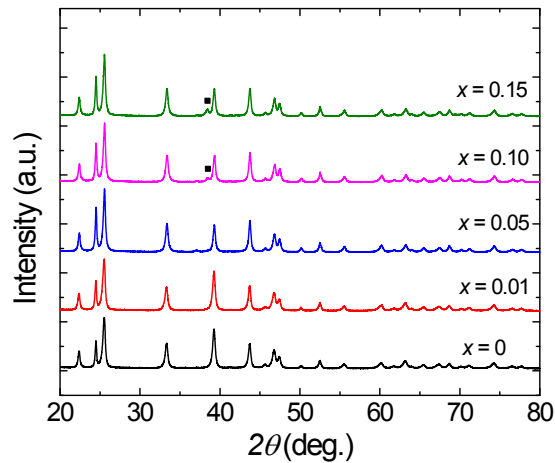


Figure S5. XRD patterns of  $\text{Mg}_{3.2-x}\text{Nb}_x\text{Sb}_{1.5}\text{Bi}_{0.49}\text{Te}_{0.01}$  ( $x = 0, 0.01, 0.05, 0.10, \text{ and } 0.15$ ).

Impurity phase of  $\text{Nb}_3\text{Sb}$  is observed when  $x > 0.05$ .

## 6. Band structure calculation

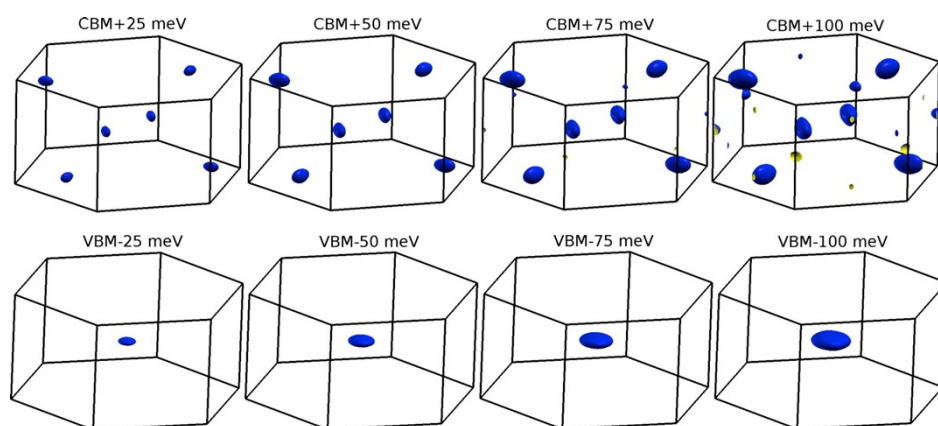


Figure S6. Calculated constant energy surfaces at 25, 50, 75, and 100 meV above conduction band minimum (CBM) and below valence band maximum (VBM), respectively.

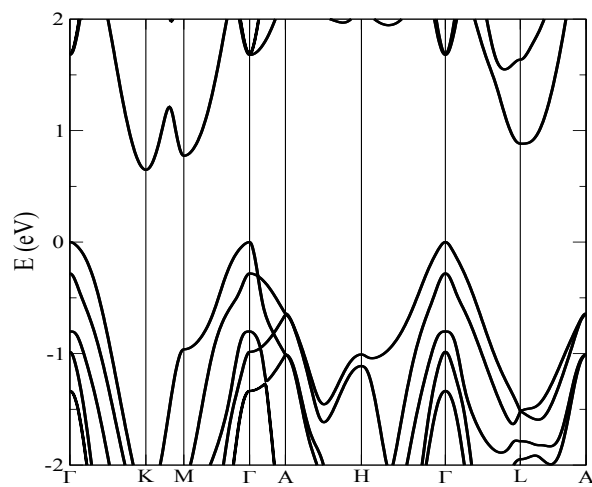


Figure S7. Calculated band structure.

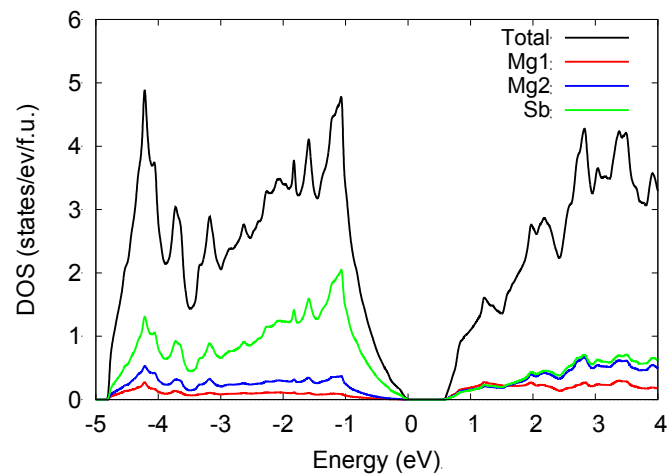


Figure S8. Calculated total DOS and partial DOS for each element.

---

## 7. Measurement for output power density

In this work the  $\text{Mg}_{3.2}\text{Sb}_{1.5}\text{Bi}_{0.49}\text{Te}_{0.01}$  and  $\text{Mg}_{3.15}\text{Nb}_{0.05}\text{Sb}_{1.5}\text{Bi}_{0.49}\text{Te}_{0.01}$  are polished to size  $\sim 2.1 \times 2.1 \text{ mm}^2$  in cross-section and  $\sim 12 \text{ mm}$  in height. Both sides of the TE leg is electroplated with copper, nickel, and gold, and soldered ( $\text{In}_{52}\text{Sn}_{48}$ , melting point  $\sim 391 \text{ K}$ ;  $\text{Pb}_{97}\text{Sn}_{1.5}\text{Ag}_{1.5}$ , melting point  $\sim 586 \text{ K}$ ) to copper plates separately. A power supply is used to supply a constant current and voltage is measured by the nanovoltmeter. K-type thermocouples are connected to copper plates to measure the temperature of both sides. The cold side copper plate is maintained at  $\sim 298 \text{ K}$  by water circulation. By changing the temperature of hot side, a series of output power density can be obtained. The experiments are performed under high vacuum (below  $10^{-6} \text{ mbar}$ ) to eliminate convection and air conduction losses.